Gas-Phase Thermochemistry of Iron Oxides and Hydroxides: Portrait of a Super-Efficient Flame Suppressant

C. Brian Kellogg* and Karl K. Irikura

Physical and Chemical Properties Division, National Institute of Standards and Technology, Gaithersburg, Maryland 20899

Received: October 29, 1998

In the search for non-ozone-depleting Halon (CF_3Br) replacements, several metals, including iron, have been identified as super-efficient flame suppressants. Although some thermochemical data exist for the species that are thought to be most important in iron's flame chemistry, a more complete and accurate characterization of the thermochemistry of iron oxides, hydrides, and hydroxides is required to improve kinetic flame models. In this investigation predicted enthalpies ($\Delta_{rxn}H_0^\circ$) and free energies ($\Delta_{rxn}G_{1500}^\circ$) of the reactions of several FeO_xH_y species in methane flames are reported. Heats of formation ($\Delta_fH_0^\circ$) for the FeO_xH_y species of interest are also recommended. The hybrid B3LYP density-functional method and the CCSD(T) coupled-cluster method are employed in conjunction with a relativistic effective core potential on the iron center and a valence triple-ζ basis on all atoms in order to characterize the relative energetics of the important species.

I. Introduction

Halons (halocarbons) have been employed extensively as fire extinguishing agents over the past three decades, but now have been phased out due to indications they may be responsible for the depletion of stratospheric ozone.[1] As a result, efficient, nontoxic flame suppression agents must be found to replace halons. In order to better understand which physical and chemical processes contribute to flame inhibition, many investigators have performed extensive empirical testing of the flame suppression of various materials. Preliminary studies of the flame inhibition properties of metals have produced dramatic results, prompting the inclusion of a large number of metals in a 1990 list of potential Halon replacements.[2] In particular, flame velocity studies indicate $Fe(CO)_5$ can be up to one hundred times more efficient a flame inhibitor than CF_3Br, the canonical extinguishing agent.[3] Very little is known, however, about the chemical mechanism by which iron achieves such impressive flame inhibition. Although iron pentacarbonyl itself is too toxic to be a useful halon replacement, understanding the reasons for its efficiency could provide valuable insight into which chemical properties are most critical to efficient flame inhibition.

The chemistry of flames is dominated by the formation of radicals through branching chain reactions. The main propagator of these reaction chains in hydrocarbon flames is the hydrogen atom. CF_3Br is thought to suppress flames through chain termination by atomic Br. In H_2 flames, for example, atomic Br enters the catalytic cycle depicted in Figure 1. The net result of each cycle is the formation of one hydrogen molecule from two hydrogen atoms. This sort of catalytic radical recombination is thought to be the main mechanism by which most chemical flame inhibitors operate.[4]

According to the studies of Reinelt and Linteris,[5] the catalytic radical destruction efficiency of $Fe(CO)_5$ is concentration dependent, with the absolute flame velocity reduction leveling off at relatively low concentrations (≈100 μg/g). On the basis of this evidence Reinelt and Linteris postulate that a highly efficient, homogeneous mechanism may dominate at lower concentrations. If such a mechanism is responsible for the flame extinction behavior observed for $Fe(CO)_5$, the fact that the effectiveness levels off at higher concentrations could be explained by the condensation of iron-containing species within the flame. The numerical simulations of Rumminger, Reinelt, Babushok, and Linteris lend further support to this model.[6] Rumminger et al. report that their kinetic simulations agree with experimental observation for low concentrations of $Fe(CO)_5$ but overpredict the flame inhibition at higher concentrations. Since their model assumes that the concentrations of gaseous iron oxides, iron hydrides, and iron hydroxides are strictly a function of the amount of iron pentacarbonyl added to the system, the overprediction of the flame suppression activity would be consistent with the formation of inactive solid particles. An earlier kinetic simulation study conducted by Babushok, Tsang, Linteris, and Reinelt explored the chemical limits of flame suppression by simulating an ideal inhibitor which scavenges H radicals and subsequently reacts with H or OH to form H_2 and H_2O at the collision rate.[7] The modeled and observed flame suppression levels for $Fe(CO)_5$ concentrations on the 10−100 μg/g level nearly match the calculated inhibition levels for the hypothetical, perfect inhibitor presented by Babushok et al.

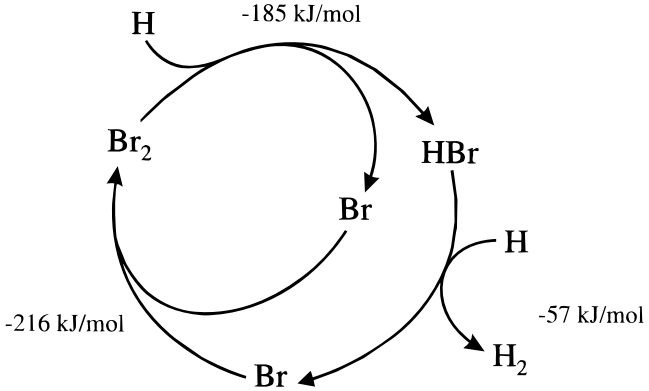

Figure 1. Catalytic cycle by which Br atoms eliminate H atoms and produce H_2. $\Delta_{rxn}G_{1500}^\circ$ (in kJ mol^{-1}) is presented for each reaction based upon $\Delta_fG_{1500}^\circ$ values taken from ref 34.

* Author to whom correspondence should be addressed.

10.1021/jp9842749 CCC: $18.00
Published on Web 02/04/1999

The iron−carbon bonds in $Fe(CO)_5$ are estimated to be no stronger than ≈170 kJ mol^{-1} and quickly break within a flame.[8] In 1974, Jensen and Jones proposed a mechanism by which iron monoxide could destroy radicals catalytically in hydrogen flames.[9] To enter their reaction cycle, atomic iron may react with molecular oxygen:

$$Fe + O_2 \rightarrow FeO_2 \quad (1)$$

and iron dioxide may subsequently react with an oxygen atom to form iron monoxide:

$$FeO_2 + O \rightarrow FeO + O_2 \quad (2)$$

The main catalytic cycle proposed by Jensen and Jones is defined by reactions 3−5:

$$FeO + H_2O \rightarrow Fe(OH)_2 \quad (3)$$

$$Fe(OH)_2 + H \rightarrow FeOH + H_2O \quad (4)$$

$$FeOH + H \rightarrow FeO + H_2 \quad (5)$$

so that two hydrogen atoms are destroyed in each cycle. Additionally, another loop is added to this cycle by the reaction

$$FeOH + H \rightarrow Fe + H_2O \quad (6)$$

though Jensen and Jones suggest that this should be a relatively minor pathway. Because of the lack of thermochemical data for some of these species it is difficult to assess whether such mechanisms could be responsible for the observed levels of flame inhibition. Similarly, a lack of accurate information about the thermal stability of related compounds such as FeOO and FeO(OH) makes it difficult to determine their role in these processes.

The simulations by Babushok et al. employed a kinetic model which was based upon reactions 1−6. The subsequent study of Rumminger and coworkers introduced a number of other reactions to the model, including a set of reactions to model the decomposition of $Fe(CO)_5$ and a set of reactions involving Fe-containing species and hydrocarbons such as CH_4, CH_3, CH_3O, and CH_3OH. Rumminger et al. found that the additional reactions did not significantly change the predicted flame suppression levels, suggesting that reactions 1−6 are central to iron's flame chemistry, while other cycles are less important.

Transition-metal compounds, especially those involving first-row transition metals, are notoriously difficult to characterize via ab initio electronic structure methods.[10] The history of ab initio studies of transition-metal-containing compounds has been chronicled in such reviews as those by Bauschlicher, Langhoff, and Partridge,[10] Siegbahn,[11] and Veillard.[12] Multireference configuration interaction (MRCI) techniques have been the most successful in predicting ground and excited-state properties for transition metal containing diatoms and triatoms. MRCI methods, however, are difficult to apply and are highly demanding computationally. The coupled-cluster method including single and double excitations and noniterative triples [CCSD(T)] has also enjoyed some success in predicting ground-state properties for transition-metal-containing species. CCSD(T) also requires large computational resources, but, in contrast to the MRCI method, does not require the careful choice of an active space since it is a single-reference method.

The most recent studies of transition metals, however, have predominantly employed density functional theory (DFT).[13] The hybrid B3LYP functional,[14−16] in particular, has become a very popular tool for investigating transition-metal-containing species. Pure DFT methods have been found to over-stabilize low-spin electronic states of transition metals in contrast to Hartree−Fock-based methods which preferentially stabilize high-spin states. This discrepancy in state-ordering stems from the different treatment of electron exchange in the two methods. Pure DFT methods replace the non-local two-electron exchange operator of the HF method with a local functional term. The hybrid B3LYP functional employs an exchange term which is a mixture of the HF exchange term and the Becke exchange term. As a result, B3LYP predictions of the energetic spacing of various spin states are often much closer to the experimental observation than either the HF or pure DFT predictions. For iron compounds, in particular, the investigations of Ricca and Bauschlicher,[17] Glukhovtsev, Bach, and Nagel[18] and Bach, Shobe, Schlegel, and Nagel[19] have employed B3LYP and produced thermochemical predictions that are thought to be accurate to within approximately 20 kJ mol^{-1}. In order to achieve similar or better accuracy with pure ab initio methods, prohibitively expensive techniques such as multi-configurational SCF and multireference configuration interaction must be employed since ordinary single-reference methods are often incapable of providing even qualitatively correct predictions for transition-metal compounds.

Several schema exist for establishing heats of formation via ab initio methods. Popular parametrized methods such as the G2[20] and BAC-MP4[21] methods require relatively modest computational resources by today's standards, but their application is limited to compounds containing main-group elements, since only compounds containing these elements were used in the parametrization of the methods. Siegbahn has proposed the PCI-80 and more general PCI-X methods which assume that a specific correlated method [typically CCSD or CCSD(T)] will recover a nearly constant fraction of the total correlation energy.[11] Pure ab initio techniques such as the atomization method of Martin[22] require considerable computational resources but are not limited to any particular region of the periodic table. Another advantage of the atomization method over parameterized methods is that the accuracy of the predicted thermodynamic quantities may be increased in a natural and logical fashion, whereas parameterized methods can only provide a single number with approximate error bars. A third strategy is to use model reactions that combine the species of interest with molecules that have well-established heats of formation. Ab initio estimates of the heat of reaction then yield the heat of formation of the compound of interest. To increase the accuracy of such a technique, it is best if the model reaction preserves the oxidation states of the constituent atoms, the total number of unpaired spins, and the types of bonds found in the reactant and product molecules.

For the iron oxides, hydrides, and hydroxides, the BAC-MP4 and G2 methods are not an option, since iron falls well outside the range of elements for which they are parameterized. The atomization approach is possible, but not practical because it would require enormous computational resources since very high levels of electron correlation are necessary to properly characterize the iron atom. The PCI-X method is, in principle, applicable for every element on the periodic table, but Siegbahn notes that the late 3d transition elements are particularly difficult, as the correlation scaling factor X must be chosen for each study.[11] As a result, model reactions are the most attractive option. Unfortunately, the gas-phase heats of formation for most iron-containing species have not been established with a high degree of certainty. The exception is $FeCl_2$, which has a

TABLE 1: Auxiliary $\Delta_f H_0^\circ$ Data, in kJ mol^{-1}, Used in Model Reactions in Table 2 and in Reactions Listed in Table 5; Data Come from the JANAF Thermochemical Tables[a] Except Where Noted Otherwise

species	$\Delta_f H_0^\circ$	species	$\Delta_f H_0^\circ$
H	216.025 ± 0.006	O	246.7 ± 0.1
OH	38.39 ± 1.21	OOH	5.0 ± 8.4
H_2O	−238.921 ± 0.042	HCl	−92.1 ± 0.2
SiH_4	43.9 ± 2.1	SiH_3Cl	−132.8 ± 8
$SiCl_2$	−168.7 ± 3.3	SiO	−101.6 ± 8.4
Si	446 ± 8	CH_3	149 ± 0.8
CH_3O	17 ± 4.0[b]	CH_3OH	−190 ± 0.2
CH_4	−66.9 ± 0.34	Fe	413.1 ± 1.3
FeCl	207 ± 7[c]	$FeCl_2$	−142 ± 4[c]

[a] Chase, M. W.; Davies, C. A.; Downey, J. R., Jr.; Frurip, D. J.; McDonald, R. A.; Syverud, A. N. *J. Phys. Chem. Ref. Data, Suppl. 1* **1985**, *14*. [b] Tsang, W. Heats of Formation of Organic Free Radicals by Kinetic Methods. In *Energetics of Organic Free Radicals*; Martinho Simões, J. A., Greenberg, A., Liebman, J. F., Eds.; (Blackie Academic and Professional: London, 1996; pp 22−58. [c] Hildenbrand, D. L. *J. Chem. Phys.* **1995**, *103*, 2634.

reasonably well-established $\Delta_f H_0^\circ$ of 142 ± 4 kJ mol^{-1}.[23] This suggests model reactions such as

$$\underline{FeO}\ (^5\Delta) + 2HCl \rightarrow FeCl_2\ (^5\Delta) + H_2O \quad (7)$$

$$\underline{Fe(OH)_2}\ (^5A) + 2HCl \rightarrow FeCl_2\ (^5\Delta) + 2H_2O \quad (8)$$

$$\underline{Fe}\ (^5D) + 2SiH_3Cl + H_2 \rightarrow FeCl_2\ (^5\Delta) + 2SiH_4 \quad (9)$$

where the underlined compound is the compound whose heat of formation we wish to predict. Si compounds are used in these reactions because of the relatively low uncertainties for the heats of formation of SiO, $SiCl_2$, SiH_3Cl, and SiH_4 (Table 1). Another reason for choosing the silicon compounds over, for example, the equivalent carbon compounds is that silicon exhibits more metallic character, and hence the nature of the bonding does not change as dramatically in each hypothetical reaction.

In this study we attempt to characterize the heats of reaction for 44 of the 54 reactions included in the kinetic model of Rumminger et al. The 10 reactions that are excluded all involve the decomposition of $Fe(CO)_5$ to form atomic iron. The 17 species involved in these reactions, 7 of which contain iron, are characterized using the B3LYP density functional method as well as the CCSD(T) method. Additionally, model reactions which involve species with well-established heats of formation are employed to establish unknown heats of formation whenever possible.

II. Methods

The B3LYP functional was used to obtain equilibrium structures and harmonic vibrational frequencies for all of the diatomic and polyatomic species of interest. In all investigations, the 10 innermost core electrons of iron were replaced with the effective core potential (ECP) derived by the Stuttgart group[24] from Dirac−Fock atomic wave functions. Russo, Martin, and Hay investigated the use of ECPs derived from atomic HF wavefunctions in conjunction with density functional theory for a variety of first-row transition-metal compounds and concluded that ECPs may be employed in DFT investigations with little loss of accuracy.[25] Although they employed only pure DFT methods in their study, Russo et al. suggest that ECPs should perform equally well for hybrid DFT methods since they apparently perform well in conjunction with the DFT and HF components separately.

Two different basis sets are employed in conjunction with the Stuttgart ECP. The smaller of the two, henceforth designated B1, consists of the (8s7p6d)/[6s5p3d] basis presented by Dolg and co-workers for Fe,[24] and the 6-311G** conventional basis for H, O, Cl, and Si.[26] For the second basis set, henceforth designated B2, only the three tightest primitive d-functions on Fe were included in the contracted d-function and two f-functions ($\alpha_1^f = 2.64$, $\alpha_2^f = 1.32$) were added to give a final contraction scheme of (8s7p6d2f)/[6s5p4d2f]. For the other elements, B2 consisted of the 6-311++G(3df,3pd) Pople-style basis.[27,28] These basis sets are nearly identical to the basis sets employed by Glukhovtsev and co-workers,[18] except that B1 employs a single polarization function for hydrogen for all compounds where Glukhovtsev employed two functions for some compounds in their smaller basis set, and B2 employs three p and one d function for H where Glukhovtsev uses only two p functions. Geometry optimizations and harmonic vibrational frequency predictions for all species of interest were performed using B1. Single-point B3LYP and CCSD(T)[29] energies were obtained at the B3LYP/B1 equilibrium geometries using B2. Both B3LYP and CCSD(T) were employed using the spin-unrestricted formalism. The CCSD(T) energies are employed as a gauge of the accuracy of the thermochemical predictions, as a large discrepancy between the B3LYP and CCSD(T) predictions suggests the need for a higher-level treatment. The Gaussian94 suite of programs was employed for all investigations.[30,31] Throughout this study, only real wave functions were employed, and so all electronic wavefunctions which are described as having either Π or Δ spatial symmetry were actually treated in a lower symmetry, but do exhibit the real, Cartesian projection of these symmetries.

B3LYP/B1 geometries and unscaled frequencies were used to compute $(H_{1500}^\circ - H_0^\circ)$ and S° for the six species using the standard thermochemical formulas.[32] Low-lying excited-state energies were taken from experiment, when available, and from B3LYP/B2 results otherwise. All vibrational degrees of freedom were treated as harmonic oscillators in thermal function computations with the exception of the OH torsional mode for $Fe(OH)_2$ which was treated as a free rotor. All data used to derive the thermal functions and their associated uncertainties are available as supplemental information. Values for the $(H_{1500}^\circ - H_0^\circ)$ and S° for all atoms and compounds not included in Table 3 were taken from the JANAF thermochemical tables.[33]

III. Results

$\Delta_f H_0^\circ$ values for the various iron-containing species of interest and the model reactions used to derive those values are presented in Table 2. The $\Delta_f H_0^\circ$ values for the auxiliary species involved in these computations are given in Table 1 along with their references. The best calculated values for $\Delta_f H_0^\circ$ presented in Table 3 are derived from the model reaction that we judged to be the most reliable. The criteria used to select the best reaction are discussed below. Since few reliable experimental data exist for the heats of formation, it is difficult to assess the accuracy of the B3LYP and CCSD(T) predictions. The lack of reliable data also impedes the application of such semi-empirical techniques as the PCI-X method. The $\Delta_f H_0^\circ$ values presented in Table 3 are the average of the B3LYP/B2 and CCSD(T)/B2 values of $\Delta_f H_0^\circ$ for the selected model reaction. This choice was made on the basis of the fact that several well-established quantities, such as the energetic separation of the d^6s^2 and d^7s^1

TABLE 2: Predicted Heats of Formation at 0 K for the Various Gaseous Iron Species of Interest As Determined by the B3LYP/B2 (A) and CCSD(T)/B2 (B) Levels of Theory[a]

reaction no.	ΔOS(Fe)	reaction	$\Delta_f H_0^\circ$ A	$\Delta_f H_0^\circ$ B
(9)	+2	$\underline{Fe}$ (^5D) + $2SiH_3Cl$ + H_2 → $FeCl_2$ ($^5\Delta$) + $2SiH_4$	417	417
(10)	+2	$\underline{Fe}$ (^5D) + 2HCl → $FeCl_2$ ($^5\Delta$) + H_2	369	358
(16)	−1	$\underline{FeCl}$ ($^6\Delta$) + SiH_4 → Fe (^5D) + SiH_3Cl + H (^2S)	204	204
(17)	0	$\underline{2FeCl}$ ($^6\Delta$) + H_2 → Fe (^5D) + $FeCl_2$ ($^5\Delta$) + 2H (^2S)	199	194
(11)	−1	$\underline{FeH}$ ($^6\Delta$) → Fe (^5D) + H (^2S)	460	451
(12)	0	$\underline{2FeH}$ ($^6\Delta$) + 2HCl → Fe (^5D) + $FeCl_2$ ($^5\Delta$) + H_2 + 2H (^2S)	460	446
(13)	0	$\underline{2FeH}$ ($^6\Delta$) + $2SiH_3Cl$ + H_2 → Fe (^5D) + $FeCl_2$ ($^5\Delta$) + $2SiH_4$ + 2H (^2S)	455	441
(14)	0	$\underline{FeH}$ ($^6\Delta$) + HCl → FeCl ($^6\Delta$) + H_2	444	436
(15)	0	$\underline{FeH}$ ($^6\Delta$) + SiH_3Cl → FeCl ($^6\Delta$) + SiH_4 + 2H (^2S)	462	454
(18)	−2	$\underline{FeO}$ ($^5\Delta$) + O (^3D) → Fe (^5D) + O_2 ($^3\Sigma_g^-$)	294	298
(7)	0	$\underline{FeO}$ ($^5\Delta$) + 2HCl → $FeCl_2$ ($^5\Delta$) + H_2O	223	250
(19)	0	$\underline{FeO}$ ($^5\Delta$) + $SiCl_2$ → $FeCl_2$ ($^5\Delta$) + SiO	228	263
(20)	−1	$\underline{FeOH}$ ($^6A'$) → Fe (^5D) + OH ($^2\Pi$)	150	132
(21)	0	$\underline{2FeOH}$ ($^6A'$) + 2HCl + H_2 → Fe (^5D) + $FeCl_2$ ($^5\Delta$) + $2H_2O$ + 2H (^2S)	87	75
(22)	0	$\underline{FeOH}$ ($^6A'$) + HCl → FeCl ($^6\Delta$) + H_2O	95	88
(25)	−4	$\underline{FeO_2}$ ($^5B_1$) + 2 H_2 → Fe (^5D) + $2H_2O$	182	147
(24)	−3	$\underline{FeO_2}$ ($^5B_1$) + HCl + H (^2S) + H_2 → FeCl ($^6\Delta$) + $2H_2O$	110	97
(23)	−2	$\underline{FeO_2}$ ($^5B_1$) + 2HCl + H_2 → $FeCl_2$ ($^5\Delta$) + $2H_2O$	103	79
(26)	0	$\underline{FeO_2}$ ($^5B_1$) + Fe (^5D) + 4HCl → $2FeCl_2$ ($^5\Delta$) + $2H_2O$	56	23
(27)	0	$\underline{FeO_2}$ ($^5B_1$) + Fe (^5D) + $2SiCl_2$ → $2FeCl_2$ ($^5\Delta$) + 2SiO	66	48
(29)	−2	$\underline{Fe(OH)_2}$ (^5A) + H_2 → Fe (^5D) + $2H_2O$	−272	−272
(28)	−1	$\underline{Fe(OH)_2}$ (^5A) + HCl + H (^2S) → FeCl ($^6\Delta$) + $2H_2O$	−288	−288
(8)	0	$\underline{Fe(OH)_2}$ (^5A) + 2HCl → $FeCl_2$ ($^5\Delta$) + $2H_2O$	−318	−328
(30)	−3	$\underline{FeO(OH)}$ ($^4A''$) + H_2 + H (^2S) → Fe (^5D) + $2H_2O$	−52	−14
(31)	−2	$\underline{FeO(OH)}$ ($^4A''$) + HCl + 2H (^2S) → FeCl ($^6\Delta$) + $2H_2O$	−68	−30
(32)	−1	$\underline{FeO(OH)}$ ($^4A''$) + 2HCl + H (^2S) → $FeCl_2$ ($^5\Delta$) + $2H_2O$	−99	−70
(33)	0	$\underline{FeO(OH)}$ ($^4A''$) + FeCl ($^6\Delta$) + 3HCl → $2FeCl_2$ ($^5\Delta$) + $2H_2O$	−130	−112

[a] Geometries and zero-point energies are predicted at the B3LYP/B1 level. Heats of formation for the underlined species are reported in kJ mol^{-1}. The overall change in the oxidation state of the iron centers from reactants to products [ΔOS] is tabulated for each reaction. Each model reaction is labeled with the reaction number from the text.

TABLE 3: The Best Calculated $\Delta_f H_0^\circ$ Values from Table 2[a]

species	best comp. model	best comp. $\Delta_f H_0^\circ$	$\Delta_f H_{298}^\circ$	Experimental $\Delta_f H_{298}^\circ$
FeH	(15)	458 ± 23	458 ± 23	510 ± 13,[b] 476 ± 8,[c] 486 ± 18[d]
FeO	(19)	246 ± 22	245 ± 22	251 ± 21,[e] 276 ± 13[f]
FeOH	(22)	91 ± 21	92 ± 21	133 ± 17,[f] 69 ± 20[g]
FeO_2	(23)	91 ± 20	91 ± 20	75 ± 21,[h] < 142 ± 20[i]
FeO(OH)	(30)	−85 ± 20	−84 ± 20	
$Fe(OH)_2$	(8)	−323 ± 20	−324 ± 20	−323 ± 2[e,j]

[a] See Discussion section in text for description of method used to obtain the best values and 1σ error bars. Available experimental numbers are presented for comparison. All values are given in kJ mol^{-1}. [b] Sallans, L.; Lane, K. R.; Squires, R. R.; Freiser, B. S. *J. Am. Chem. Soc.* **1985**, *107*, 4379. [c] Schultz, R. H.; Armentrout, P. B. *J. Chem. Phys.* **1991**, *94*, 2262. [d] Miller, A. E. S.; Miller, T. M.; Morris, R. A.; Viggiano, A. A.; Vandoren, J. M.; Paulson, J. F. *Int. J. Mass Spectrom. Ion Processes* **1993**, *123*, 205. [e] Chase, M. W.; Davies, C. A.; Downey, J. R., Jr.; Frurip, D. J.; McDonald, R. A.; Syverud, A. N. *J. Phys. Chem. Ref. Data, Suppl. 1* **1995**, *14*. [f] Murad, E. *J. Chem. Phys.* **1980**, *73*, 1381. [g] Jensen, D. E.; Jones, G. A. *J. Chem. Soc. Faraday Trans.* **173**, *69*, 1448. [h] Hildenbrand, D. L. *Chem. Phys. Lett.* **1975**, *34*, 352. [i] Jacobson, D. B.; Freiser, B. S. *J. Am. Chem. Soc.* **1986**, *108*, 27. [j] Value is listed as approximate, and reported error bars are not an adequate gauge of uncertainty.

manifolds of the Fe atom, the ionization energy of the iron atom, and T_0 for the $^6\Delta$ state of FeH, are all reproduced by the average of the B3LYP/B2 and CCSD(T)/B2 predictions (see below). We have assigned error bars to our theoretical heats of formation which reflect the uncertainty in the experimental heats of formation as well as a 20 kJ mol^{-1} uncertainty in the computational prediction that is based on previous applications of DFT to iron thermochemistry and our agreement with the available experimental values.[17−19] In cases where the B3LYP/B2 and CCSD(T)/B2 $\Delta_f H_0^\circ$ values differed by more than 40 kJ mol^{-1}, the computational uncertainty was assumed to be half of the difference between the two predictions rather than 20 kJ mol^{-1}. The square root of the sum of the squares of the respective uncertainties is presented as an approximate 1σ error bar in Tables 3, 4, and 5. This uncertainty is intended to reflect a 2/3 confidence interval. However, the computational uncertainty is only a rough estimate since the errors it represents are primarily systematic.

For some of the species in this study, there has been no experimental assignment of a ground-state spin and spatial symmetry. In these cases we adopted the B3LYP prediction of the lowest-lying electronic state. Although the limited accuracy of the B3LYP method precludes the definitive characterization of the electronic ground state, the uncertainty in the ground state energy due to this assumption should fall well within the prescribed confidence interval.

Bond dissociation energies predicted for a variety of Fe−H, Fe−O, and Fe−OH bonds are presented in Table 4. These are not computed directly but using our best computed heats of formation from Table 3. Experimental values for the bond strengths are also provided in Table 4. Only experimental values that were directly measured or calculated from heats of formation measured by the same methods by the same group are quoted in Table 4. Reaction enthalpies ($\Delta_{rxn}H_0^\circ$) and free energies of reaction at 1500 K ($\Delta_{rxn}G_{1500}^\circ$) for 47 reactions involving iron compounds and radical flame species are presented in Table 5. Again, the values presented are based upon the best computed values from Table 3.

A. Atomic Fe. Many electronic structure methods have a difficult time accurately reproducing the relative stability of the d^6s^2 and d^7s configurations of atomic iron. The J-averaged separation between the lowest electronic state manifolds for these configurations, the ^5D and ^5F states, respectively, is 84.3

TABLE 4: Bond Strengths (in kJ mol^{-1}) for a Variety of Fe−O and Fe−OH Bonds Species of Interest as Determined by the Recommended Values for $\Delta_f H_0^\circ$ (Table 3)[a]

bond	D_0°	experimental D_{298}°
Fe−H	171 ± 23	119 ± 13,[b] 153 ± 8,[c] 143 ± 18[d]
Fe−O	414 ± 22	408 ± 21,[e] 383 ± 13,[f] 405 ± 13[g]
Fe−OH	361 ± 21	328 ± 17,[f] 382 ± 20[h]
FeO−H	370 ± 31	359 ± 21[f]
OFe−O	401 ± 30	428 ± 24[g]
OFe−OH	369 ± 30	
HOFe−O	423 ± 29	
OFeO−H	392 ± 29	
HOFe−OH	454 ± 29	
HOFeO−H	455 ± 29	

[a] Uncertainty for computational values represent 1σ error bars. Available experimental numbers are presented for comparison. [b] Sallans, L.; Lane, K. R.; Squires, R. R.; Freiser, B. S. *J. Am. Chem. Soc.* **1985**, *107*, 4379. [c] Schultz, R. H.; Armentrout, P. B. *J. Chem. Phys.* **1991**, *94*, 2262. [d] Miller, A. E. S.; Miller, T. M.; Morris, R. A.; Viggiano, A. A.; Vandoren, J. M.; Paulson, J. F. *Int. J. Mass Spectrom. Ion Processes.* **1993**, *123* 205. [e] Chase, M. W.; Davies, C. A.; Downey, J. R., Jr.; Frurip, D. J.; McDonald, R. A.; Syverud, A. N. *J. Phys. Chem. Ref. Data, Suppl. 1* **1995**, *14*. [f] Murad, E. *J. Chem. Phys.* **1980**, *73*, 1381. [g] Hildenbrand, D. L. *Chem. Phys. Lett.* **1975**, *34*, 352. [h] Jensen, D. E.; Jones, G. A. *J. Chem. Soc. Faraday Trans.* **1973**, *69*, 1448.

kJ mol^{-1} with the ^{5}D state as the lower of the two.[34] The B3LYP method predicts a separation of 51.3 kJ mol^{-1} with basis B1 and 57.2 with basis B2, overstabilizing the d^7s configuration. This is much better than the Hartree−Fock method which predicts separations of 337.3 and 199.9 kJ mol^{-1} with B1 and B2, respectively. Like HF, CCSD(T) overstabilizes the d^6s^2 configuration, giving a prediction of 116.2 kJ mol^{-1} with basis B2. Since the CCSD(T) bias is opposite to the B3LYP bias, CCSD(T) predictions of reaction energetics should provide a good check for B3LYP energetics and the difference between the two can serve as an estimate of the inherent uncertainty in the predictions.

Many of the reactions studied in this investigation involve a change in iron's oxidation state. The ability of B3LYP and CCSD(T) to treat such changes may be roughly gauged by their ability to reproduce iron's first ionization potential. B3LYP/B1 and B3LYP/B2 give values of 783 and 784 kJ mol^{-1}, respectively, approximately 20 kJ above the experimental value of 761 kJ mol^{-1}.[35] CCSD(T)/B2 gives an ionization potential of 743 kJ mol^{-1}, 18 kJ mol^{-1} below the experimental value. Once again the two methods display opposing biases, with the experimental value nearly the average of the B3LYP and CCSD(T) values.

It is possible to obtain an estimate of the heat of formation of neutral atomic iron through the use of model reactions such as

$$\mathrm{Fe}\ (^5\mathrm{D}) + 2\mathrm{HCl} \rightarrow \mathrm{FeCl_2}\ (^5\Delta) + \mathrm{H_2} \qquad (10)$$

and reaction 9. Since the heat of formation of atomic iron is well-established (415 kJ mol^{-1}),[33] this scheme can provide a test of the reliability of such model reactions to establish unknown heats of formation. Reactions 9 and 10 are not expected to produce very accurate estimates of $\Delta_f H_0^\circ$ since they both involve atomic iron, a known stumbling block for both DFT and ab initio methods, and the oxidation state of iron changes from 0 to II from reactants to products. The results presented in Table 2 indicate that a wide range of values for heats of formation may be obtained depending upon the model reaction employed. Reaction 9 is expected to give somewhat more reliable results since the Fe−Cl bonds should be more closely approximated by Si−Cl bonds than by H−Cl bonds. This expectation is confirmed by the good agreement of both the DFT and CCSD(T) values of $\Delta_f H_0^\circ$ using reaction 9 as compared to the poor agreement obtained with reaction 10 (see Table 2).

TABLE 5: Predicted Heats of Reaction at 0 K ($\Delta_{rxn}H_0^\circ$) and Change in Gibbs Free Energy at 1500 K ($\Delta_{rxn}G_{1500}^\circ$) for Reactions of Gaseous Iron Species with Flame Radicals[a]

	reaction	$\Delta_{rxn}H_0^\circ$	$\Delta_{rxn}G_{1500}^\circ$
(9)	$Fe + O_2 \rightarrow FeO_2$	−356 ± 28	−115 ± 30
(2)	$FeO_2 + O \rightarrow FeO + O_2$	−58 ± 36	−53 ± 38
(3)	$FeO + H_2O \rightarrow Fe(OH)_2$	−330 ± 30	−95 ± 33
(4)	$Fe(OH)_2 + H \rightarrow FeOH + H_2O$	−40 ± 29	−61 ± 32
(5)	$FeOH + H \rightarrow FeO + H_2$	−62 ± 31	−40 ± 32
(6)	$FeOH + H \rightarrow Fe + H_2O$	−133 ± 21	−114 ± 22
(11)	$Fe + H \rightarrow FeH$	−171 ± 23	40 ± 23
(19)	$Fe + OH \rightarrow FeOH$	−361 ± 21	−126 ± 22
(34)	$FeO(OH) + CH_3 \rightarrow FeO_2 + CH_4$	−74 ± 35	−130 ± 38
(35)	$FeO(OH) + CH_4 \rightarrow Fe(OH)_2 + CH_3$	23 ± 29	−43 ± 33
(36)	$Fe + O \rightarrow FeO$	−414 ± 22	−168 ± 23
(37)	$Fe + O_2 \rightarrow FeO + O$	79 ± 22	82 ± 23
(38)	$FeO + O \rightarrow FeO_2$	−435 ± 36	−197 ± 38
(39)	$FeO + H \rightarrow FeOH$	−370 ± 31	−156 ± 32
(40)	$FeO + OH \rightarrow FeO(OH)$	−369 ± 30	−30 ± 33
(41)	$FeO + H \rightarrow Fe + OH$	−10 ± 22	−30 ± 23
(42)	$FeO + CH_3 \rightarrow Fe + CH_3O$	36 ± 23	71 ± 23
(43)	$FeO + H_2 \rightarrow Fe + H_2O$	−71 ± 22	−74 ± 23
(44)	$FeO_2 + H \rightarrow FeO(OH)$	−358 ± 35	−125 ± 38
(45)	$FeO_2 + H \rightarrow FeO + OH$	12 ± 36	0 ± 38
(46)	$FeO_2 + OH \rightarrow FeOH + O_2$	−5 ± 35	−11 ± 37
(47)	$FeOH + O \rightarrow FeO(OH)$	−413 ± 29	−162 ± 32
(48)	$FeOH + OH \rightarrow Fe(OH)_2$	−454 ± 29	−179 ± 32
(49)	$FeOH + OH \rightarrow FeO + H_2O$	−124 ± 31	−84 ± 32
(50)	$FeOH + O \rightarrow Fe + O_2H$	80 ± 23	103 ± 24
(51)	$FeOH + O \rightarrow FeO + OH$	−54 ± 31	−41 ± 32
(52)	$FeOH + CH_3 \rightarrow FeO + CH_4$	−62 ± 31	−98 ± 32
(53)	$FeO(OH) + H \rightarrow Fe(OH)_2$	−455 ± 29	−215 ± 33
(54)	$FeO(OH) + CH_3 \rightarrow FeO + CH_3OH$	−9 ± 30	35 ± 33
(55)	$FeO(OH) + H \rightarrow FeO + H_2O$	−125 ± 30	−120 ± 33
(56)	$FeO(OH) + H \rightarrow FeO_2 + H_2$	−74 ± 35	−71 ± 38
(57)	$FeO(OH) + H \rightarrow FeOH + OH$	−1 ± 29	−36 ± 32
(58)	$FeO(OH) + OH \rightarrow FeOH + O_2H$	142 ± 31	139 ± 33
(59)	$FeO(OH) + OH \rightarrow FeO_2 + H_2O$	−102 ± 29	−85 ± 33
(60)	$FeO(OH) + O \rightarrow FeO + O_2H$	88 ± 31	97 ± 34
(61)	$FeO(OH) + O \rightarrow FeO_2 + OH$	−66 ± 35	−73 ± 38
(62)	$FeO(OH) + O \rightarrow FeOH + O_2$	−71 ± 29	−88 ± 32
(63)	$Fe(OH)_2 + OH \rightarrow FeO(OH) + H_2O$	−39 ± 29	−26 ± 33
(64)	$Fe(OH)_2 + CH_3 \rightarrow FeOH + CH_3OH$	76 ± 29	93 ± 32
(65)	$FeH + O \rightarrow FeOH$	−614 ± 31	−364 ± 32
(66)	$FeH + O_2 \rightarrow FeO(OH)$	−534 ± 31	−276 ± 33
(67)	$FeH + O_2 \rightarrow FeOH + O$	−120 ± 31	−114 ± 32
(68)	$FeH + H \rightarrow Fe + H_2$	−261 ± 23	−236 ± 23
(69)	$FeH + O \rightarrow Fe + OH$	−253 ± 23	−238 ± 24
(70)	$FeH + OH \rightarrow Fe + H_2O$	−323 ± 23	−281 ± 24
(71)	$FeH + CH_3 \rightarrow Fe + CH_4$	−261 ± 23	−295 ± 24

[a] Values are based upon recommended $\Delta_f H_0^\circ$ values from Table III for iron compounds and experimental values for FeCl, $FeCl_2$, atomic iron and all other compounds from Table 1. $\Delta_f H_0^\circ$ and $\Delta_{rxn}G_{1500}^\circ$ are reported in kJ mol^{-1}. Note that some reactions are the reverse of the reactions as they appear in the text. Uncertainty for computational values represent 1σ error bars.

B. FeH. The $^4\Delta$ state of FeH has been identified as the ground state,[36,37] while the *a* $^6\Delta$ state is known to be 23.27 ± 0.66 kJ mol^{-1} (1945 ± 55 cm^{-1}) above the ground state.[38,39] Most electronic structure methods have a difficult time getting even the ordering of these two states correct due to the fact that the $^4\Delta$ state requires extremely high levels of electron correlation in order to be properly characterized.[10]

Our B3LYP/B1 and B3LYP/B2 predictions of the T_0 for the $^6\Delta$ state are about 26 kJ mol^{-1} too high at 52 and 50 kJ mol^{-1}, respectively. The B3LYP/B1 computed bond lengths for the

two states, 1.557 and 1.658 Å for the $^4\Delta$ and $^6\Delta$ states, respectively, are in modest agreement with the available experimental numbers, 1.61 and 1.77 Å.[38,40] The CCSD(T)/B2 prediction is 26 kJ mol^{-1} too low, $T_0 = -3$ kJ mol^{-1}. Once again, although the absolute predictions of each method separately are in significant error, the average of the two predictions is very close to the experimental value.

Since the $^4\Delta$ state is so difficult to treat properly and T_0 for the $^6\Delta$ state is well-established, it should be possible to obtain more reliable estimates of $\Delta_f H_0^\circ$ through the use of model reactions involving the $^6\Delta$ state. We used three different model reactions to predict the heat of formation of FeH:

$$\underline{\text{FeH}}\ (^6\Delta) \rightarrow \text{Fe}\ (^5\text{D}) + \text{H}\ (^2\text{S}) \quad (11)$$

$$2\underline{\text{FeH}}\ (^6\Delta) + 2\text{HCl} \rightarrow \text{Fe}\ (^5\text{D}) + \text{FeCl}_2\ (^5\Delta) + \text{H}_2 + \text{H}\ (^2\text{S}) \quad (12)$$

$$2\underline{\text{FeH}}\ (^6\Delta) + 2\text{SiH}_3\text{Cl} + \text{H}_2 \rightarrow \text{Fe}\ (^5\text{D}) + \text{FeCl}_2\ (^5\Delta) + 2\text{SiH}_4 + 2\text{H}\ (^2\text{S}) \quad (13)$$

The hydrogens in reactions 12 and 13 are present to make the reactions isogyric (spin conserving). In setting up these reactions we have assumed that iron is in oxidation state Fe(I). Ideally, we would like to use model reactions which incorporate only Fe(I) species. Hildenbrand has reported $\Delta_f H_0^\circ$ 207 ± 7 kJ mol^{-1} for FeCl ($^6\Delta$),[23] and so the reactions

$$\underline{\text{FeH}}\ (^6\Delta) + \text{HCl} \rightarrow \text{FeCl}\ (^6\Delta) + \text{H}_2 \quad (14)$$

$$\underline{\text{FeH}}\ (^6\Delta) + \text{SiH}_3\text{Cl} \rightarrow \text{FeCl}\ (^6\Delta) + \text{SiH}_4 \quad (15)$$

should also provide reasonable estimates of $\Delta_f H_0^\circ$ FeH. Unfortunately, Hildenbrand's reported value for $\Delta_f H_0^\circ$ FeCl is not in very good agreement with the high-level CCSD(T) predictions of Bauschlicher[41] or the B3LYP investigations of Bach et al.[19] To evaluate the utility of such reactions and the experimental $\Delta_f H_0^\circ$ for FeCl, we used the model reactions

$$\underline{\text{FeCl}}\ (^6\Delta) + \text{SiH}_4 \rightarrow \text{Fe}\ (^5\text{D}) + \text{SiH}_3\text{Cl} + \text{H}\ (^2\text{S}) \quad (16)$$

$$2\underline{\text{FeCl}}\ (^6\Delta) + \text{H}_2 \rightarrow \text{Fe}\ (^5\text{D}) + \text{FeCl}_2\ (^5\Delta) + 2\text{H}\ (^2\text{S}) \quad (17)$$

As illustrated in Table 2, the $\Delta_f H_0^\circ$ (FeCl) values predicted by B3LYP/B2 and CCSD(T)/B2 show exceptional agreement with one another and are in good agreement with Hildebrand's value. As a result of this favorable agreement, we have chosen to use FeCl as a reference compound for determining the heats of formation of iron(I) compounds.

The heats of formation deduced from model reactions (11−15) are given in Table 2. Since the average of the CCSD(T) and B3LYP values for other properties gives better agreement with experiment than either alone, we suggest that the best estimate for the heat of formation is an average of the two values. There is no fundamental reason why the average of energies predicted by these methods should provide accurate answers, and this relationship will be discussed more below.

Bond dissociation energies predicted for a variety of Fe−H, Fe−O, and Fe−OH bonds are presented in Table 4. As stated in the Methods section, these are not computed directly, as in equation 11, but using our best computed heats of formation from Table 3. Experimental estimates of D_0° (Fe−H) vary rather widely; values from 108 to 184 kJ mol^{-1} have been reported.[18] It is therefore difficult to determine which method gives a closer match to experiment since both B3LYP and CCSD(T) give D_0° values that fall in or near this range.

Several low-lying electronic states were located for many of the iron compounds, often separated by fewer than four kJ mol^{-1}. Since these energetic separations are well-below the assumed accuracy of the methods which we have employed, we cannot make any definitive assignment of the ground electronic state in these cases. The final heat of formation predictions, however, should not differ dramatically for a different choice of ground state when their separation is so small, and so resolution of the true ground state is not essential for this study.

C. FeO. The ground state of FeO is experimentally well-established as $^5\Delta$.[40] In contrast to FeH, theoretical characterizations of FeO have been in relative harmony with the experimental observations.[43,44] The B3LYP/B1 predictions of the equilibrium bond length and harmonic vibrational frequency are 1.615 Å and 882 cm^{-1}, respectively. These predictions agree favorably with the experimental values of 1.57 Å for r_e and 965 cm^{-1} for ν_0.[40]

The contrast between the B3LYP/B1 bond-length errors for FeO (+0.05 Å) and FeH (−0.05 Å) points toward a potential inequity in treatment of the (I) and (II) oxidation states of iron. As a result, predicted enthalpies for reactions involving a change in iron's oxidation state could include an over-stabilization of reactants or products. This is a general concern in the field of computational thermodynamics and is discussed in more detail below.

For FeO, three different model reactions were employed:

$$\underline{\text{FeO}}\ (^5\Delta) + \text{O}\ (3\text{P}) \rightarrow \text{Fe}\ (^5\text{D}) + \text{O2}\ (^3\Sigma_g^-) \quad (18)$$

$$\underline{\text{FeO}}\ (^5\Delta) + \text{SiCl}_2 \rightarrow \text{FeCl}_2\ (^5\Delta) + \text{SiO} \quad (19)$$

and reaction 7. While none of these reactions maintains truly equivalent bond types, reaction 19 comes the closest to being homodesmic and should give relatively reliable predictions.

D. FeOH. Iron hydroxide has been studied far less than either FeO or FeH, and very little is known definitively about this species. In their study of iron-containing species, Glukhovtsev et al.[18] predicted a ^{6}A′ ground state with an Fe−OH bond strength of 304 kJ mol^{-1}, in marginal agreement with Murad's measurement of 322 ± 17 kJ mol^{-1}.[42] At the B3LYP/B2 level, we find the ^{6}A′ state to be the ground state with a directly calculated bond strength of 306 kJ mol^{-1}, and at the CCSD(T)/B2//B3LYP/B1 level, this increases to 324 kJ mol^{-1}, in much better agreement with the experimental value. Our investigations also located low-lying ^{6}A″ and ^{4}A″ states which are 1.3 and 3.8 kJ mol^{-1}, respectively, above the ^{6}A′ state at the B3LYP/B2 level.

Reactions similar to reacitons 11 and 12 may be employed to establish the heat of formation of FeOH:

$$\underline{\text{FeOH}}\ (6\text{A}') \rightarrow \text{Fe}\ (^5\text{D}) + \text{OH}\ (^2\Pi) \quad (20)$$

$$2\underline{\text{FeOH}}\ (6\text{A}') + 2\text{HCl} \rightarrow \text{Fe}\ (^5\text{D}) + \text{FeCl}_2\ (^5\Delta) + 2\text{H}_2\text{O} + 2\text{H}\ (^2\text{S}) \quad (21)$$

As with FeH, we also used a model reaction which involves FeCl ($^6\Delta$):

$$\underline{\text{FeOH}}\ (6\text{A}') + \text{HCl} \rightarrow \text{FeCl}\ (^6\Delta) + \text{H}_2\text{O} \quad (22)$$

E. FeO_2. FeO_2 has been studied rather extensively in the past few years both experimentally[44,45] and theoretically.[44,45,46] The

calculations of Cao, Duran, and Solà employed CCSD(T) at HF optimized geometries to obtain relative energetics for the various electronic states of the dioxide (O−Fe−O), superoxide (Fe−O−O), and dioxygen (Fe−O_2) isomers of FeO_2.[46] Not surprisingly, their predictions differ rather significantly from those of the DFT investigations of Andrews et al.[44] The highest levels of theory applied by Cao et al. predict that the $^1A_1$ state of the dioxide is the most stable state and isomer. In contrast, Andrews and coworkers found that the B3LYP method predicts a $^5B_2$ ground state for the dioxide isomer and a close-lying $^3B_1$ state (T_0 = 10.1 kJ mol^{-1}), but conclude that the $^3B_1$ state is the ground state for that isomer on the basis of agreement between the predicted and observed isotopic vibrational shifts for that state.

Our own investigations of FeO_2 were focused on finding the overall lowest state among the various possible geometries and spin multiplicities. We considered states with $D_{\infty h}$, $C_{\infty v}$, C_{2v}, and C_s geometries and with quintet, triplet, and singlet spin multiplicities. Our calculations differ somewhat from those of Andrews et al. in that they employed an all-electron basis. The main conclusions, however, are very similar. Our DFT investigations predicted a bent, C_{2v} $^5B_2$ ground state with the $^3B_1$ state just 6 kJ mol^{-1} higher. The predicted Fe−O bond lengths for the $^5B_2$ and $^3B_1$ states are 1.605 and 1.584 Å, respectively, while the corresponding O−Fe−O bond angles are 117.8° and 139.9°. The lowest superoxide state is the $^5A'$ state at 162 kJ mol^{-1} above the $^5B_2$ state. In all computations of heat of reaction and heat of formation involving FeO_2, the $^5B_2$ state was assumed to be the ground state. Because we are mainly concerned with energetics, identifying the true ground state is not essential since our predictions are only accurate to approximately 20 kJ mol^{-1}. Definitive characterization of the relative energies of the various isomers and electronic states of FeO_2 by purely ab initio methods (i.e., without relying on comparisons with experimentally observed vibrational isotopic ratios) would require robust multireference methods such as MRCISD, CASSCF/MRCI, or CAS/PT2.

FeO_2 has an iron center with a nominal oxidation state of (IV). Unfortunately, no iron(IV) species have well-established heats of formation, so reactions such as

$$\underline{FeO_2}\ (^5B_2) + 2HCl + H_2 \rightarrow FeCl_2\ (^5\Delta) + 2H_2O \quad (23)$$

$$\underline{FeO_2}\ (^5B_2) + HCl + H_2 \rightarrow FeCl\ (^6\Delta) + 2H_2O \quad (24)$$

$$\underline{FeO_2}\ (^5B_2) + 2H_2 \rightarrow Fe\ (^5D) + 2H_2O \quad (25)$$

must be employed. Alternatively, we may use comproportionation reactions such as

$$\underline{FeO_2}\ (^5B_2) + Fe\ (^5D) + 4HCl \rightarrow 2FeCl_2\ (^5\Delta) + 2H_2O \quad (26)$$

$$\underline{FeO_2}\ (^5B_2) + Fe\ (^5D) + 2SiCl_2 \rightarrow 2FeCl_2\ (^5\Delta) + 2SiO \quad (27)$$

where the two iron centers on the reactant side change oxidation state by an equal amount but in opposite directions. This sort of reaction should eliminate systematic biases associated with changes in the iron oxidation state. The spread between the B3LYP and CCSD(T) $\Delta_f H_0^\circ$ values varies a great deal among these reactions (Table 2). The $\Delta_f H_0^\circ$ prediction based on reaction 27 should be more reliable based on the quality of the model reaction.

F. FeO(OH) and $Fe(OH)_2$. There has been no direct experimental observation of either FeO(OH) or $Fe(OH)_2$, though these species have been proposed as possible participants in a variety of catalytic processes.[42,9] The bond strengths and heats of formation of the closely related compounds MnO(OH) and $Mn(OH)_2$ have been recently reported by Hildenbrand and Lau.[47] Their reported values establish a hierarchy for Mn−OH and Mn−O bond strengths:

$$\text{Mn−OH} < \text{OMn−OH} < \text{HOMn−OH}$$

$$(322\ \text{kJ mol}^{-1}) \quad (372\ \text{kJ mol}^{-1}) \quad (439\ \text{kJ mol}^{-1})$$

$$\text{Mn−O} < \text{HOMn−O} < \text{OMn−O}$$

$$(372\ \text{kJ mol}^{-1}) \quad (427\ \text{kJ mol}^{-1}) \quad (485\ \text{kJ mol}^{-1})$$

Hildenbrand and Lau go on to observe that the relative magnitudes of these bond strengths are consistent with the values which have been observed for other transition-metal systems.

For FeO(OH), we considered doublet, quartet, and sextet states as candidates for the ground state, and explored Fe(III) and Fe(I) (Fe−OOH) geometries. At the B3LYP/B2 level of theory, the $^6A'$ Fe(III) state is the lowest in energy, with the $^4A'$ and $^4A''$ states nearly degenerate at ∼7 kJ mol^{-1} higher. The two quartet states exhibit very nearly linear O−Fe−O segments while the sextet state exhibits a bond angle of 160° and all three states exhibit an Fe−O−H bond angle between 132° and 134°. None of the peroxy isomers was close enough in energy at the B3LYP/B2 level to be considered as a contender for the ground state, with the lowest-energy peroxy state, the $^6A'$ state, 280 kJ mol^{-1} above the ground state. In all computations of FeO(OH) bond strengths, heats of formation, and reaction enthalpies, the $^6A'$ state was assumed to be the ground state.

Quintet, triplet, and singlet spin states and C_{2v}, C_{2h}, C_2, and C_s geometries were all considered for $Fe(OH)_2$. In all cases, the FeO_2 segment was linear or nearly linear and Fe−O−H angles were approximately 130°. At the DFT/B2 level, the ^5A C_2 state was found to have the lowest electronic energy, but the $^5A_1$ C_{2v} state and $^5A'$ C_{2h} states are only 0.4 and 0.5 kJ mol^{-1} higher. These three states differ only by a torsion of one of the O−H groups and a slight bend in the O−Fe−O angle for the ^5A state (175.5°). The $^5A_1$ and $^5A'$ states are both transition states between the right-handed and left-handed C_2 structures, but ZPVE corrections make all of the structures nearly degenerate, with the $^5A_1$ and $^5A'$ states slightly lower than the ^5A C_2 state. The torsional motion of the OH segments experiences only a very small barrier (less than 0.5 kJ mol^{-1} with B3LYP/B2). The lowest triplet state is 53 kJ mol^{-1} higher than the ^5A state at the DFT/B2 level. For all bond strength, enthalpy of reaction, and heat of formation calculations the ^5A state was assumed to be the ground state of $Fe(OH)_2$.

In the $Fe(OH)_2$ molecule, iron is in a (II) oxidation state, and so a model reaction involving $FeCl_2$ as the product molecule for iron is best. Therefore reaction 8 which is isogyric and includes $FeCl_2$ is ideal, though the isogyric reactions

$$\underline{Fe(OH)_2}\ (^5A) + HCl + H\ (^2S) \rightarrow FeCl\ (^6\Delta) + 2H_2O \quad (28)$$

$$\underline{Fe(OH)_2}\ (^5A) + H_2 \rightarrow Fe\ (^5D) + 2H_2O \quad (29)$$

should also produce fairly reliable $\Delta_f H_0^\circ$ values. Similar model reactions may be employed to establish the heat of formation of trivalent FeO(OH):

$$\underline{\text{FeO(OH)}}\ (^4\text{A}'') + \text{H}_2 + \text{H (2S)} \rightarrow \text{Fe}\ (^5\text{D}) + 2\text{H}_2\text{O} \quad (30)$$

$$\underline{\text{FeO(OH)}}\ (^4\text{A}'') + \text{HCl} + 2\text{H (2S)} \rightarrow \text{FeCl}\ (^6\Delta) + 2\text{H}_2\text{O} \quad (31)$$

$$\underline{\text{FeO(OH)}}\ (^4\text{A}'') + 2\text{HCl} + \text{H (2S)} \rightarrow \text{FeCl}_2\ (^5\Delta) + 2\text{H}_2\text{O} \quad (32)$$

As with FeO_2, a comproportionation reaction may also be applied:

$$\underline{\text{FeO(OH)}}\ (^4\text{A}'') + \text{FeCl}\ (^6\Delta) + 3\text{HCl} \rightarrow 2\text{FeCl}_2\ (^5\Delta) + 2\text{H}_2\text{O} \quad (33)$$

The Fe−OH bond strengths predicted by both DFT and CCSD(T) follow a trend similar to that observed for the Mn−OH bond strengths in the study of Hildenbrand and Lau (Table 3). The ratio of the predicted OFe−O and Fe−O bond strengths, however, is much lower than would be expected from the experimental Mn−O bond strength trends.

IV. Discussion

A. Recommended $\Delta_f H_0^\circ$ Values. As Table 2 illustrates, the predicted heat of formation can vary a great deal depending on the model reaction employed to obtain it. Also, there is serious discrepancy between the CCSD(T) and B3LYP predictions of $\Delta_f H_0^\circ$ for many of the model reactions. To extract a single meaningful estimate of $\Delta_f H_0^\circ$ for each compound, it is necessary to guess which reaction will give the most accurate heat of formation and subsequently decide on a single number based on the B3LYP and CCSD(T) values.

Criteria for selecting the best model reaction among the available options are fairly well-established. The model reactions involving FeCl or $FeCl_2$ and silicon compounds should, in principle, give the most reliable $\Delta_f H_0^\circ$ values. Reactions involving a change in iron's oxidation state should be avoided if possible, since both of the methods employed in this study tend to give an unbalanced treatment to the two iron centers in such reactions. Changes in the oxidation states of the other constituents of the reactants can also compromise the quality of a model reaction, and should be avoided when possible. The gas-phase heats of formation for $FeCl_2$ and FeCl are experimentally well-established,[23] and so model reactions for FeO, $Fe(OH)_2$, FeH, and FeOH can be designed which maintain iron's oxidation state. Since FeO_2 and FeO(OH) are formally Fe(IV) and Fe(III), respectively, no model reactions that maintain iron's oxidation state may be constructed. Instead, we used comproportionation reactions, which involve the simultaneous oxidation and reduction of two separate iron centers to give products which have the same oxidation state. These reactions should, in principle, remove systematic errors associated with a change in oxidation state. The heats of reaction presented in Table 2 indicate a preferential stabilization of the lower oxidation states of iron. The model reactions for FeO_2, FeO(OH), and $Fe(OH)_2$, in particular, show that progressively lower oxidation state reference compounds lead to progressively higher values for $\Delta_f H_0^\circ$. The low value of the confidence intervals relative to the spread of the $\Delta_f H_0^\circ$ values for the various model reactions for FeO_2, FeO(OH), and $Fe(OH)_2$ reflects the quality of model reactions which preserve the oxidation state and the sensitivity of the predicted $\Delta_f H_0^\circ$ value to the quality of the model reaction. Our best calculated heats of formation are summarized in Table 3.

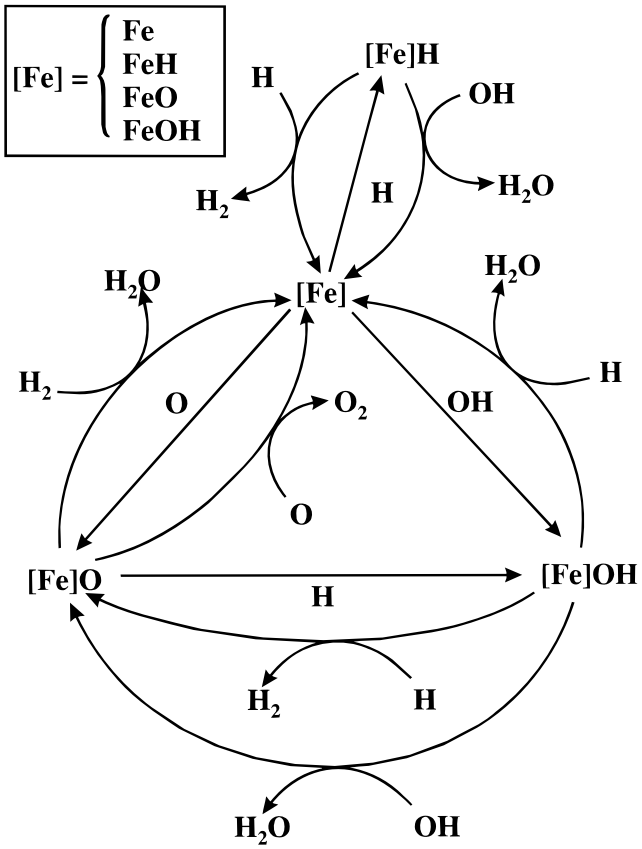

Figure 2. Schematic representation of different classes of reactions which may contribute to iron's super-efficient flame suppression ability through the catalytic recombination of radical species.

B. Chemical Consequences of Thermodynamic Findings. To be an effective catalyst for radical recombination, a molecule must be able to effectively bind radicals, but not so tightly that they can not be abstracted by other radicals to form stable, closed shell species. Figure 2 illustrates some cycles that may be envisioned for iron in the flame environment. On the basis of the heats of reaction in Table 5, a number of catalytic cycles that involve only exothermic reactions may be added to the cycles proposed by Jensen and Jones. In fact, most of the catalytic cycles that involve the seven iron species in our study are thermodynamically favorable at hydrocarbon flame temperatures (≈1500 K) meaning that they are either exothermic or weakly endothermic at 0 K ($\Delta_{rxn} H_0^\circ < 10$ kJ mol^{-1} l). One of the original aims of this study was to make a rough survey of the various reactions of iron in the presence of H, O, and OH radicals in order to determine which reactions and reactive cycles would not be competitive solely on the basis of their thermodynamics. If the list of potentially important reactions could be shortened, then effort could be focused on the kinetics of the remaining reactions. However, as it turned out, many of the reactions and cycles are exothermic and very few reactions may be eliminated.

Typical hydrocarbon flame temperatures are between 1000 and 2000 K, and so $\Delta_{rxn} H_0^\circ$ may not be the best criterion for the identification of reactions which are not thermodynamically reasonable. The free energies of reaction at 1500 K ($\Delta_{rxn} G_{1500}^\circ$) for the reactions considered in this study are presented in Table 5. The $(G_{1500}^\circ - G_0^\circ)$ and S_{1500}° values used to compute the $\Delta_{rxn} G_{1500}^\circ$ values values are tabulated in the Supporting Information. With few exceptions, the $\Delta_{rxn} G_{1500}^\circ$ values are very close to the $\Delta_{rxn} H_0^\circ$ values. Reactions which involve changes in molecularity show the most dramatic differences. But, even in

these cases, no qualitative changes are introduced, so that almost all the steps in all conceivable radical scavenging cycles involve a decrease in the Gibbs free energy.

A few of the reactions included in Table 5 are endergonic, however. Most of the reactions that do exhibit a positive $\Delta_{rxn}G^\circ_{1500}$ value can be broken down into two major categories: reactions of iron centers with methyl radical[42,54,64] and reactions that evolve O_2H.[50,58,60] Though most of the methyl radical pathways that lead to CH_3OH or CH_3O are thermodynamically unfavorable, some of the other reactions considered by Rumminger et al. that lead instead to CH_4[52,71] are exergonic. Additionally, similar reactions of iron species with CH_3 radicals

$$FeO(OH) + CH_3 \rightarrow FeO_2 + CH_4 \quad (34)$$

$$Fe(OH)_2 + CH_3 \rightarrow FeO(OH) + CH_4 \quad (35)$$

are also exoergic and should be included in future kinetic simulations. Since neither of these categories of reactions is central to the assumed flame inhibition mechanism, the results of kinetic models will probably not be significantly changed as a result of these findings. Excluding the O_2H-producing reactions may increase slightly the modeled flame inhibition by iron compounds since it reduces the production of free radicals.

The $\Delta_f H^\circ_0$ predictions presented in Table 3 generally agree with most of the thermodynamic data adopted by Rumminger et al. in their kinetic simulation.[6] The data used by Rumminger and coworkers come primarily from either the JANAF tables,[33] the NIST webbook,[48] or the IVTANTHERMO database.[49] One notable exception is the heat of formation for FeO(OH), which Rumminger et al. assume to be 18 kJ mol^{-1} [49] while we obtain $\Delta_f H^\circ_0$ -85 ± 20 kJ mol^{-1}.

C. General Comments, Recommendations for Future Investigations. Computational thermochemistry of transition metals is still extremely difficult. The complexity of the electronic structure of transition metals precludes the use of many of the more affordable ab initio methods which have met with a great deal of success in predicting the thermochemistry of light main-group elements. The lack of highly reliable experimental data hinders the formulation of accurate parameterized methods akin to the G2 method.

Density-functional methods have recently enjoyed a great deal of success in predicting transition-metal thermochemistry, but these methods, too, have some major limitations. B3LYP predictions, for example, are often in reasonable agreement with experiment, but there is no way of systematically improving their accuracy or of gauging their reliability in any specific case. DFT methods are still plagued by many of the problems that foil ab initio investigations of transition metals: slow convergence of the electronic density, a large number of local minima, improper characterization of spin state orderings, and imbalanced treatment of the different oxidation states of each metal center.

The CCSD(T) method is considered to be less sensitive to the quality of the reference wavefunction than are other single-reference ab initio methods. This makes the method quite attractive for transition metals since multireference methods are often prohibitively expensive for such systems due to the large active space which is required for an adequate multi-reference treatment. Unfortunately, the CCSD equations are often quite difficult to converge for transition-metal compounds.[46] In our investigation we maintained CCSD convergence criteria of 10^{-5} Hartrees for the energy and 10^{-7} for the wavefunction amplitudes. These convergence criteria translate to an error of approximately 0.1 kJ mol^{-1} in the absolute energy. Even with these relatively loose criteria, 40−60 iterations of the CCSD equations were required for convergence for most of the iron species. With more stringent criteria, convergence was often not reached in over one hundred iterations.

In order for computational transition-metal thermochemistry to become both more reliable and more straightforward, it is necessary to have more reliable benchmarks. In the absence of experimental data, the methods and machinery now exist to perform very-high level ab initio *studies* on small transition-metal compounds to achieve very accurate and reliable predictions of fundamental thermochemical properties. These sorts of studies on diatomic and triatomic transition-metal species can provide information about the convergence of thermochemical properties with respect to correlation effects, both dynamical and non-dynamical, as well as the data required to produce more practical and affordable parametrized schema for obtaining accurate thermochemical data.

For the systems studied in this investigation, a more accurate assessment of the thermodynamics of the reactions of interest will probably not qualitatively change the conclusion that almost all catalytic radical recombination cycles are thermodynamically accessible at flame temperatures. Instead, future efforts should focus on the relative rates of various reactions in order to assess the importance of the various possible contributing cycles. The kinetic models of Babushok et al. assume that all of the relevant reactions proceed without any barrier. Even relatively crude estimates of the reaction rates would help to refine the current picture, and possibly to eliminate some pathways from further consideration. A rough estimate of the relative rates of reactions 5 and 6, for example, would provide a better idea of the importance of the cycle which is entered through reaction 6. This is a much more challenging task than obtaining thermodynamic data, but is important to understanding iron's behavior in hydrocarbon flames.

V. Conclusions

This investigation has characterized the heats of formation of the gas-phase species FeH, FeO, FeOH, FeO_2, FeO(OH), and $Fe(OH)_2$ by means of a combination of DFT and ab initio electronic structure calculations and model thermochemical reactions. On the basis of these heats of formation, almost all of the reactions involving these species and potentially contributing to chemical flame suppression are found to be exergonic at 1500 K. A more accurate assessment of the heats of formation of the iron species will require high-level ab initio techniques such as MRCI or CAS-MP2, but the qualitative conclusions are not likely to change. Further refinement of the current model of iron's super-efficient flame suppression abilities will require information about the kinetics of individual reactions either from experiment or from computational investigations that apply more rigorous methods than those applied in this study.

Computational studies of iron are quite challenging. The density of states, significant multi-reference character, ambiguity of spin state, slow convergence, and dearth of definitive experimental data all make it difficult to computationally characterize iron compounds with a great deal of confidence. The heats of formation predicted in this study vary a great deal depending upon the model reaction used to predict $\Delta_f H^\circ_0$. High-level benchmark studies of the thermochemistry of simple iron compounds such as FeH, FeO, and FeOH are probably possible with modern computational methods and resources. Such studies would help to elucidate the convergence properties of more affordable electronic structure methods and guide future efforts to characterize the thermochemistry of transition-metal containing species in general.

Acknowledgment. We thank Wing Tsang for suggesting this interesting topic and Valeri Babushok for very helpful discussions. We are also grateful to Marc Nyden and T. Daniel Crawford for their reviews of the manuscript.

Supporting Information Available: B3LYP/B1-computed equilibrium geometries and harmonic vibrational frequencies for the ground states of all species considered, the computed geometries and vibrational freqencies of all of the excited states for iron-containing species which exhibited more than one low-lying state, absolute energies computed at the B3LYP/B1, B3LYP/B2, and CCSD(T)/B2 levels are also reported for all species considered. Values of $S°$ (1500) and $[H°(1500) - H°(0)]$ used to compute $\Delta_{rxn}G°_{1500}$ and associated uncertainties (4 pages print/PDF). See any current masthead page for ordering information and Web access instructions.

References and Notes

(1) Molina, M. J.; Rowland, F. S. *Nature* **1974**, *249*, 810.

(2) Pitts, W. M.; Nyden, M. R.; Gann, R. G.; Mallard, W. G.; Tsang, W. *NIST Technical Note no. 1279: Construction of an exploratory list of chemicals to initiate the search for halon alternatives*; National Institute of Standards and Technology, Gaithersburg, MD, 1990.

(3) Jost, W.; Bonne, U.; Wagner, H. G. *Chem. Eng. News* **1961**, *39*, 79.

(4) *Halon Replacements: Technology and Science*; Miziolek, A. W., Tsang, W., Eds.; ACS Symposium Series 611; American Chemical Society: Washington, DC, 1995.

(5) Reinelt, D.; Linteris, G. T. *26th Symposium on Combustion*; The Combustion Institute: Pittsburgh, 1996.

(6) Rumminger, M. D.; Reinelt, D.; Babushok, V.; Linteris, G. T. *Combust. Flame*, accepted for publication.

(7) Babushok, V.; Tsang, W.; Linteris, G.; Reinelt, D. *Combust. Flame*, accepted for publication.

(8) Lewis, K. E.; Golden, D. M.; Smith, G. P. *J. Am. Chem. Soc.* **1984**, *106*, 3905.

(9) Jensen, D. E.; Jones, G. A. *J. Chem. Phys.* **1974**, *60*, 3421.

(10) Bauschlicher, C. W., Jr.; Langhoff, S. R.; Partridge, H. In *Modern Electronic Structure Theory*; Yarkony, D. R., Ed.; World Scientific: London, 1995.

(11) Siegbahn, P. E. M. *Adv. Chem. Phys.* **1993**, *93*, 333.

(12) Veillard, A. *Chem. Rev.* **1991**, *91*, 743.

(13) Kohn, W.; Becke, A. D.; Parr, R. G. *J. Phys. Chem.* **1996**, *100*, 12974.

(14) Becke, A. D. *J. Chem. Phys.* **1993**, *98*, 5648.

(15) Lee, C.; Yang, W.; Parr, R. G. *Phys. Rev. B* **1988**, *37*, 785.

(16) Stephens, P. J.; Devlin, F. J.; Chabalowski, C. F.; Frisch, M. J. *J. Phys. Chem.* **1994**, *98*, 11623.

(17) Ricca, A.; Bauschlicher, C. W. *Theo. Chim. Acta* **1995**, *92*, 123.

(18) Glukhovtsev, M. N.; Bach, R. D.; Nagel, C. J. *J. Phys. Chem.* **1997**, *101*, 316.

(19) Bach, R. D.; Shobe, D. S.; Schlegel, H. B.; Nagel, C. J. *J. Phys. Chem.* **1995**, *100*, 8770.

(20) Curtiss, L. A.; Raghavachari, K.; Trucks, G. W.; Pople, J. A. *J. Chem. Phys.* **1991**, *94*, 7221.

(21) Melius, C. F.; Zachariah, M. R. In *Computational Thermochemistry*; Irikura, K. K., Frurip, D. J., Eds.; ACS Symposium Series 677; American Chemical Society, Washington, DC, 1998.

(22) Martin, J. M. L. In *Computational Thermochemistry* Irikura, K. K.; Frurip, D. J., Eds.; ACS Symposium Series 677; American Chemical Society, Washington, DC, 1998.

(23) Hildenbrand, D. L. *J. Chem. Phys.* **1995**, *103*, 2634.

(24) Dolg, M.; Wedig, U.; Stoll, H.; Preuss, H. *J. Chem. Phys.* **1987**, *86*, 866.

(25) Russo, T. V.; Martin, R. L.; Hay, P. J. *J. Am. Chem. Soc.* **1995**, *99*, 17085.

(26) Krishnan, R.; Binkley, J. S.; Seeger, R.; Pople, J. A. *J. Chem. Phys.* **1980**, *72*, 650.

(27) Clark, T.; Chandrasekhar, J.; Spitznagel, G. W.; Schleyer, P. V. R. *J. Comp. Chem.* **1983**, *4*, 294.

(28) Frisch, M. J.; Pople, J. A.; Binkley, J. S. *J. Chem. Phys.* **1984**, *80*, 3265.

(29) Raghavachari, K.; Trucks, G. W.; Pople, J. A.; Head-Gordon, M. *Chem. Phys. Lett.* **1989**, *157*, 479.

(30) Frisch, M. J.; Trucks, G. W.; Schlegel, H. B.; Gill, P. M. W.; Johnson, B. G.; Robb, M. A.; Cheeseman, J. R.; Keith, T. A.; Petersson, G. A.; Montgomery, J. A.; Raghavachari, K.; Al-Laham, M. A.; Zakrzewski, V. G.; Ortiz, J. V.; Foresman, J. B.; Peng, C. Y.; Ayala, P. Y.; Wong, M. W.; Andres, J. L.; Replogle, E. S.; Gomperts, R.; Martin, R. L.; Fox, D. J.; Binkley, J. S.; Defrees, D. J.; Baker, J.; Stewart, J. P.; Head-Gordon, M.; González, C.; Pople, J. A. *Gaussian 94 (Revision D.3)*; Gaussian, Inc.: Pittsburgh, 1995.

(31) Certain commercial materials and equipment are in this paper in order to specify procedures completely. In no case does such identification imply recommendation or endorsement by the National Institute of Standards and Technology, nor does it imply that the material or equipment identified is necessarily the best available for the purpose.

(32) Irikura, K. K. In *Computational Thermochemistry*; Irikura, K. K., Frurip, D. J., Eds.; ACS Symposium Series 677; American Chemical Society: Washington, DC, 1998.

(33) Chase, M. W.; Davies, C. A.; Downey, J. R., Jr.; Frurip, D. J.; McDonald, R. A.; Syverud, A. N. *J. Phys. Chem. Ref. Data, Suppl. 1* **1985**, *14*.

(34) Moore, C. E . Atomic Energy Levels, *Nat. Bur. Stand. (US) circ.* **1949**, *467*.

(35) Sugar, J.; Corliss, C. *J. Phys. Chem. Ref. Data* **1985**, *14*, Supplement No. 2.

(36) Phillips, J. G.; Davis, S. P.; Lindgreen, B.; Balfour, W. J. *Astrophys. J. Suppl. Ser.* **1987**, *65*, 721.

(37) Bauschlicher, C. W.; Langhoff, S. R. *Chem. Phys. Lett.* **1988**, *145*, 205.

(38) Stevens, A. E.; Feigerle, C. S.; Lineberger, W. C. *J. Chem. Phys.* **1983**, *78*, 5420.

(39) Carter, R. T.; Steimle, T. C.; Brown, J. M. *J. Chem. Phys.* **1993**, *99*, 3166.

(40) Huber, K. P.; Herzberg, G. Constants of Diatomic Molecules (data prepared by J. W. Gallagher and R. D. Johnson, III). In *NIST Chemistry WebBook, NIST Standard Reference Database Number 69*, March 1998; Mallard, W. G., Linstrom, P. J., Eds.; March 1998, National Institute of Standards and Technology, Gaithersburg MD, 20899 (http://webbook.nist.gov).

(41) Bauschlicher, C. W., Jr. *Chem. Phys.* **1996**, *211*, 163.

(42) Murad, E. *J. Chem. Phys.* **1980**, 1381.

(43) Krauss, M.; Stevens, W. J. *J. Chem. Phys.* **1985**, *82*, 5584.

(44) Andrews, L.; Chertihin, G. V.; Ricca, A.; Bauschlicher, C. W., Jr. *J. Am. Chem. Soc.* **1996**, *118*, 467.

(45) Chertihin, G. V.; Saffel, W.; Yustein, J. T.; Andrews, L.; Neurock, M.; Ricca, A.; Bauschlicher, C. W., Jr. *J. Phys. Chem.* **1996**, *100*, 5261.

(46) Cao, S.; Duran, M.; Solà, M. *Chem. Phys. Lett.* **1997**, *274*, 411.

(47) Hildenbrand, D. L.; Lau, K. H. *J. Chem. Phys.* **1994**, *100*, 8377.

(48) *NIST Chemistry WebBook, NIST Standard Reference Database Number 69*, March 1998; Mallard, W. G., Linstrom, P. J., Eds.; National Institute of Standards and Technology, Gaithersburg, MD 20899 (http://webbook.nist.gov).

(49) *NIST Special Database 5. IVTANTHERMO-PC*; Gurvich, L. V., Ed.; NIST, Gaithersburg, MD 20899 (Database is developed at the Institute of High Temperature, Russian Academy of Science, Moscow).